

## APPLICATION OF NASTRAN FOR STRESS ANALYSIS

## OF LEFT VENTRICLE OF THE HEART\*

Y. C. Pao  
University of Nebraska-Lincoln  
Lincoln, Nebraska

E. L. Ritman  
Mayo Graduate School of Medicine  
Rochester, Minnesota

H. C. Wang  
IBM Corporation  
Endicott, New York

## SUMMARY

Knowing the stress and strain distributions in the left ventricular wall of the heart is a prerequisite for the determination of the muscle elasticity and contractility in the process of assessing the functional status of the heart. NASTRAN has been applied for the calculation of these stresses and strains and to help in verifying the results obtained by the computer program FEAMPS which was specifically designed for the plane-strain finite-element analysis of the left ventricular cross sections. Adopted for the analysis are the true shape and dimensions of the cross sections reconstructed from multi-planar x-ray views of a left ventricle which was surgically isolated from a dog's heart but metabolically supported to sustain its beating. A preprocessor has been prepared to accommodate both FEAMPS and NASTRAN, and it has also facilitated the application of both the triangular element and isoparametric quadrilateral element versions of NASTRAN. The stresses in several crucial regions of the left ventricular wall calculated by these two independently developed computer programs are found to be in very good agreement. Such confirmation of the results is essential in the development of a method which assesses the heart performance.

---

\*This work was supported in part by research grants HL4664, HL3532, and RR7 from the National Institutes of Health, and by the Engineering Research Center, University of Nebraska-Lincoln.

## INTRODUCTION

Structurally speaking, human and animal hearts are very complex not only in geometry but also in material characteristics. The finite element method therefore presents itself as an effective tool for analyzing the stresses and strains in the hearts. In order to assess whether or not a human or animal heart is functioning normally, it is necessary that the working characteristic of its left ventricular wall muscle (myocardium) be adequately ascertained, for it is the contraction of the left ventricular myocardium that pumps the oxygenated blood to circulate in the body. For the investigation of the left ventricle of the heart alone (not to be involved with the other chambers, right ventricle, and left and right atria), experiments of surgically isolated but metabolically supported, beating left ventricles of dogs are often prepared so that the dynamic changes of the shape and dimensions of the cross sections of the left ventricles during cardiac cycles can be recorded on videotape and by use of reconstruction techniques involving multiplanar x-ray projections or ultrasonic echoes of the cross sections (ref. 1).

The reconstruction technique using x-ray is schematically illustrated in Fig. 1. For a certain cross section of interest, a number of x-ray projections are taken by rotating the cross section with a chosen angle increment about its normal axis. The shape and dimensions of the cross section can then be reconstructed by use of algebraic algorithms (ref. 2). With a life supporting system (Fig. 2) for the isolated left ventricle of a dog experiment, any desired anatomic site selected at 0.7 mm intervals along the entire apical-to-basal axis of the ventricle can be reconstructed. Figure 3 shows a sample rectangular array of 35 apical-to-basal cross sections at a certain instant of a cardiac cycle. Further details and discussion of the reconstruction and data collection techniques are given in an internal publication (ref. 3), which is available upon request.

During relaxation (diastolic) phase of a cardiac cycle, the myocardium extends as the blood fills into the left ventricle. Based on the values of the left ventricular pressure and volume concomitantly recorded during the dog experiment, the history of the external work being done to the left ventricle can be calculated. Meanwhile, the finite element method can be applied for the analysis of the reconstructed instantaneous shapes of the left ventricular cross sections to determine the stresses and strains in the wall muscle and consequently the change of the strain energies. Upon relating the external work and the strain energies, the dependency of the elastic stiffness of the myocardium on the chamber pressure can then be estimated.

While the calculation of the external work is straightforward, it is for the calculation of the stresses and strains in the left ventricular cross sections that this paper reports the application of NASTRAN as a verifier for the plane-strain finite-element computer program FEAMPS which was specifically developed for the study of the left ventricles.

## LEFT VENTRICLE MODELS AND FEAMPS

Since the thin-walled shell model was found to be adequate only for calculating the mean stresses across the wall thickness of the left ventricle, a number of thick-walled models have been proposed for obtaining the variation of the wall stresses (ref. 4). Most of the thick-walled models approximated the geometry of the left ventricle as a shell of revolution, either as a circular hollow cylinder, hollow sphere, or hollow prolate spheroid, all having uniform wall thickness. When biplane silhouettes of the left ventricle could be taken by application of the roentgen-, cine- and videodensitometry techniques (ref. 5), it became possible to incorporate some of the dimensions, such as the variations of wall thickness and chamber radii, of the left ventricle into the thick-walled models to determine the wall stresses by axisymmetric finite-element analysis. Now the advent of cross-sectional reconstruction from multiplanar x-ray views enables the thick-walled models of the left ventricle to be further improved by adopting the true shape and dimensions of the left ventricular cross sections.

However, the 35 apical-to-basal cross sections shown in Fig. 3 were obtained by a reconstruction system using only one x-ray source and one detector. The system requires the position and geometry of the left ventricle to be kept constant throughout successive cardiac cycles. This "stationarity" requirement is a serious disadvantage to be overcome by use of a spatial reconstruction system which will have multiple x-ray sources and multiple detectors. At present, the available data include (1) the dynamic changes of the cross-sectional shapes and dimensions at a few sites along the apical-to-basal axis of the left ventricle but are complete for several cardiac cycles, and (2) the shapes and dimensions for all apical-to-basal cross sections of the left ventricle but only at a few crucial instants of cardiac cycles. So these data suffice to investigate the cross-sectional behavior but not the ultimate three-dimensional analysis of the left ventricle.

FEAMPS is an abbreviation for Finite-Element Analysis of Myocardium by Plane-Strain Theory. The left ventricle is approximated as a hollow thick-walled cylinder with uniform cross section having the shape and dimensions reconstructed from multiplanar x-ray views. When the cylinder is subjected to uniform chamber pressure, it is assumed that all cross sections will deform identically. By looking at the silhouette shown in Fig. 4 constructed from stacking all cross sections in Fig. 3, it appears that plane-strain analysis should give a reasonably good prediction of the cross-sectional behavior in the vicinity of the base of the left ventricle.

It has been well established that the left ventricular myocardium is fibrous. Several investigations of the left ventricular wall with fibrous material properties had been reported (refs. 6,7). However, only scattered data are available regarding the changes of the fiber directions during cardiac cycles; the results of these investigations remain to be verified by more thorough experiments. FEAMPS follows the approach of assuming the left ventricle as a homogeneous, isotropic and elastic medium and proceeds to evaluate the effective elastic stiffness for such an equivalent model (refs. 8,9). Since the effective elastic stiffness is to be inversely determined on the basis of the

work-energy principle described in the Introduction, its value is assumed to be equal to 1 in the incremental-loading analysis of FEAMPS. Regarding the other material constant, Poisson's ratio, of the left ventricular myocardium, the issue whether it should be assumed equal to 0.415 (ref. 10) or nearly incompressible equal to 0.49 (ref. 11) is still not yet settled. So the results for both values will be discussed.

## FORMATION AND ANALYSIS OF ELEMENTS

Figures 5(a) and 5(b) show a typical change of the shape and dimensions of a cross section near the base of the left ventricle reconstructed from multi-planar x-ray views during the early and ending stages of the diastole of a cardiac cycle, respectively. The diastolic phase is the resting period of the heart during which the relaxed left ventricular chamber is filling with blood and the wall muscles are passive and extended. The two-dimensional in-plane triangular elements of FEAMPS are generated by adopting 9 nodes across the wall thickness and 30 nodes around the perimeter of a reconstructed cross section. Additional elements may be necessary for the papillary muscle at certain levels within the ventricle. Figure 5(c) illustrates that the end-diastolic cross section shown in Fig. 5(b) is partitioned into 508 triangular elements using 290 nodes, of which 20 are for the formation of the 28 triangular elements for the peninsulalike papillary muscle.

The only input data required for FEAMPS are the coordinates of 30 pairs of points on the inner (endocardial) and outer (epicardial) boundaries of the cross section, plus additional pairs if necessary for the papillary muscle. A preprocessor which consists of several subroutines has been prepared to carry out the sequential numbering and calculation of the coordinates of all nodes, to compose the interconnected triangular elements by defining their respective constituent nodes, and to generate the nodal external loads. Plot subroutines are also made available for drawing of only the borders of the cross section or the partitioning pattern of the cross section either with or without the labelling of the node and element numbers.

The plane-strain finite-element analysis of FEAMPS follows closely the procedures delineated in Zienkiewicz's book (ref. 12). The displacements at any point within the triangular element are assumed as linear polynomials of its coordinates. This results in constant strains throughout the element. For saving computer storage spaces, the structural stiffness matrix is formulated in rectangular form by taking advantage of symmetry and discarding all of the zero elements that are on the outside of the diagonal band. In order to handle such a rectangular coefficient matrix, the Gauss-Jordan elimination method has been accordingly modified for the solution of the nodal displacements. This approach has reduced the computer storage core requirement for the structural stiffness matrix from 580x580 to 580x22 floating words in the analysis of the end-diastolic cross section partitioned as shown in Fig. 5(c). In case that further reduction of core storage in the computer is necessary, the zero elements inside the diagonal band of the structural stiffness matrix may also be discarded and all nonzero elements compacted into a vector, and the Gauss-Seidel iteration method can be applied for the solution of the nodal displacements (ref. 13).

Since the left ventricular cross sections are subjected to uniform internal pressure only on the inner (endocardial) boundary and there are no boundary constraints at all, the nodal displacements determined by machine computation may contain the superposition of a free body motion. To ascertain whether the sometimes very large free body motion will introduce significant errors in the subsequent calculation of the cross-sectional stresses, studies of the cross section with added fictitious boundary conditions have been conducted. More details on these studies are presented in the Discussion of Numerical Results.

FEAMPS also has the built-in provisions for the calculation of the nodal stresses by averaging the stresses of the adjoining elements, the extrapolation of the stresses for improved accuracy at the boundary nodes, the calculation of the strain energies, and for various plottings of the stress distributions of the cross section. Figure 6 displays a sample plot of the nodal circumferential stress distribution (normalized with respect to the uniform internal pressure) of the end-diastolic cross section with the exclusion of the almost uniformly compressed papillary muscle. Full details and computer program listing of FEAMPS are given in ref. 3. Nevertheless, the above synopsis should suffice for the discussion of the present paper.

#### APPLICATION OF NASTRAN

Attempts have been made to apply NASTRAN Rigid Format I to the two-dimensional plane-strain static analysis of the reconstructed left ventricular cross sections. With the availability of the FEAMPS preprocessor, preparatory works that can be expedited are the generation of the coordinates of the nodes, the division of the cross section into either triangular TRMEM or quadrilateral QMEM1 elements, and the conversion of the uniform internal pressure on the inner (endocardial) boundary of the cross section into equivalent concentrated loads at the endocardial nodes.

As has been mentioned in the preceding section, there are no boundary constraints at all in the plane-strain analysis of the left ventricular cross sections. Test runs are necessary for the determination of acceptable fictitious points of support which can be adopted as the constraints data for the SPC1 cards and will not introduce additional external loading. For instance, in the analysis of the cross section shown in Fig. 5(c), the decision to constrain node 6 in both the x and y directions and node 19 in the y direction was based on the verification by the printout, via SPCFORCE request, that the reactive forces at these two nodes were insignificantly small relative to the external loads at the endocardial nodes.

Since the left ventricle is assumed as a homogeneous, isotropic and elastic medium, the MAT2 cards specifying the material properties were prepared with the values of the Young's modulus,  $E$ , equal to 1 and the Poisson's ratio,  $\nu$ , equal to 0.415 and 0.49, same as for the FEAMPS cases.

The extreme stresses are known to occur along the inner boundary of the left ventricular cross section; the four regions of primary concern have been

particularly pointed out in Fig. 7 to facilitate the comparison study of the FEAMPS and NASTRAN results. These regions are the inner borders of the posterior, septal, anterior and free walls in the vicinities of nodes 247, 253, 258 and 264, respectively. Figure 8 gives a close-up view of these four regions with the node and element numbers indicated.

## DISCUSSION OF NUMERICAL RESULTS

Level 15.5 was used to generate all NASTRAN results reported herein. Table 1 shows that for  $\nu=0.415$ , the values of the principal stresses (normalized with respect to the chamber pressure) in the end-diastolic cross section determined by FEAMPS and NASTRAN are almost identical when both used triangular elements. The last two columns of Table 1 reveal that the principal stresses in a quadrilateral element are very close to the average values of those of the two adjacent triangular elements which have been combined to form the quadrilateral element. Since the number of the elements is reduced to half for the QDMEM1 analysis but the computer time is about doubled, the TRMEM analysis was selected for further studies.

For  $\nu=0.415$  but for the early diastolic cross section shown in Fig. 5(a), Table 2 is presented to depict the effect of imposing fictitious boundary constraints to the cross section on the principal stresses. It is clearly indicated that restricting the x-displacement  $u$  of node 6 and the y-displacement  $v$  of nodes 6 and 19 causes no significant change to the values of the stresses. It also helps to demonstrate that the free body motion of the cross section which may result by FEAMPS analysis will not alter the values of the stresses.

The cases of treating the left ventricle as a nearly incompressible material with  $\nu=0.49$  have also been investigated. Table 3 summarizes the normalized principal stresses for both the early and end diastolic cross sections shown in Figs. 5(a) and 5(b). The results exemplify the changes of the stresses during the diastolic phase of a cardiac cycle. As in Tables 1 and 2, these results obtained by FEAMPS and NASTRAN are in very good agreement.

Since FEAMPS has a feature for calculating the nodal stresses, the normalized principal stress distributions through the wall thickness at the four regions of concern during early and end diastole have been obtained and are presented in Fig. 9. It is noteworthy that some compressive circumferential stresses may develop at the innermost (0% of wall thickness in Fig. 9) myocardial layer in the septal and free walls where the curvature are small and sometimes even turn convex inward. Because other axisymmetric models of the left ventricle assumed cross sections to be of annular shape, in no portion of the cross section could the wall be curved inward. As a consequence, no compressive circumferential stress in the left ventricular wall had ever been determined by these models.

## CONCLUDING REMARKS

The evaluation of the cross-sectional elastic stiffness (ref. 14) of the left ventricle during diastole depends in large measure on the accuracy of the values of the stresses and strains in the cross section. So it is indeed reassuring that these values can be confirmed by FEAMPS and NASTRAN.

This comparison study has also proved the applicability of NASTRAN for the plane-strain analysis of the left ventricular cross sections. Certainly, the other capabilities of NASTRAN can further help resolve some of the problems connected with the ongoing research of the three-dimensional analysis of the left ventricle, for which a special-purpose computer program is being developed. In the computer program, the true three-dimensional geometry of the left ventricle determined by the multiplanar x-ray views of its cross sections will be utilized and the analysis by treating the myocardium as a fibrous material using adjusted elastic stiffnesses and incremental loading will be incorporated.

It may also be anticipated that NASTRAN will contribute to the ultimate dynamic analysis of the left ventricle which will consider, among others, the effects of the myocardial contraction, the dynamics of the heart valves, and the interaction of the blood flow in the left ventricular chamber.

## ACKNOWLEDGEMENT

We would like to thank Dr. Earl H. Wood for his encouragement and assistance throughout this project, Dr. Richard A. Robb for the reconstruction of the cross sections and Dr. David Donald for the surgical preparation of the isolated left ventricle. Their thanks are also extended to Mrs. Sharon Zahn, Mrs. Jean Frank and her coworkers at Mayo, and Mr. John L. Nikkila and Mrs. Louise Simmons at UNL for providing computer programming assistance and/or preparing the manuscript and illustrations.

## REFERENCES

1. Robb, R. A., Greenleaf, J. F., Ritman, E. L., Johnson, S. A., Sjostrand, J. D., Herman, G. T., and Wood, E. H.: Three-Dimensional Visualization of the Intact Thorax and Contents, A Technique for Cross-Sectional Reconstruction from multiplanar X-Ray Views. Computers and Biomedical Research, Vol. 7, 1974, pp. 395-418.
2. Gordon, R., and Herman, G. T.: Reconstruction of Pictures from Their Projections. Communications of the Association for Computing Machinery, Vol. 14, 1971, pp. 759-768.
3. Pao, Y. C., Robb, R. A., and Ritman, E. L.: Plane-Strain Finite-Element Analysis of Reconstructed Left Ventricular Cross Sections. Technical

Report UNL/MAYO 7501, University of Nebraska-Lincoln, 1975. Presented at the Sixth Annual Meeting of the Biomedical Engineering Society, New Orleans, April 11-12, 1975.

4. Pao, Y. C., Ritman, E. L., and Wood, E. H.: Finite-Element Analysis of Left Ventricular Myocardial Stresses. Journal of Biomechanics, Vol. 7, 1974, pp. 469-477.
5. Ritman, E. L., Sturm, E., and Wood, E. H.: A Biplane Roentgen Videometry System for Dynamic (60/second) Studies of the Shape and Size of Circulatory Structures, Particularly the Left Ventricle. pp. 179-211 in Roentgen-, Cine- and Videodensitometry. Fundamentals and Applications for Blood Flow and Heart Volume Determination (Edited by Heintzen, P. H.), Georg Thieme Verlag, Stuttgart, 1971.
6. Janz, R. F., and Grimm, A. F.: Finite-Element Model for the Mechanical Behavior of the Left Ventricle. Circulation Research, Vol. 30, 1972, pp. 244-252.
7. Streeter, D. D., Jr., and Hanna, W. T.: Engineering Mechanics for Successive States in Canine Left Ventricular Myocardium, I. Cavity and Wall Geometry. II. Fiber Angle and Sarcomere Length. Circulation Research Vol. 33, 1973, pp. 639-664.
8. Pao, Y. C., and Ritman, E. L.: An Energy Method for Evaluating the Global Young's Modulus of Left Ventricular Myocardium in the Passive State. Technical Report UNL/MAYO 7502, University of Nebraska-Lincoln, 1975.
9. Ghista, D. N., Sandler, H., and Vayo, W. H.: Elastic Modulus of the Human Intact Left Ventricle--Determination and Physiological Interpretation. Medical and Biological Engineering, Vol. 13, 1975, pp. 151-161.
10. Ross, A. L.: A Finite Element Computer Program for Nonlinear Structural Analysis of the Heart. General Electric Report 72SD213, King of Prussia, Pennsylvania, 1972.
11. Janz, R. F., Kubert, B. R., Moriarty, T. F., and Grimm, A. F.: Deformation of the Diastolic Left Ventricle--II. Nonlinear Geometric Effects Journal of Biomechanics, Vol. 7, 1974, pp. 509-516.
12. Zienkiewicz, O. C.: The Finite Element Method in Engineering Science, McGraw-Hill, New York, 1971.
13. Pao, Y. C., and Ritman, E. L.: On Storage, Retrieval, and Gauss-Seidel Iteration Involving Nonzero Elements of a Sparse Stiffness Matrix Compacted as a Vector. Computers and Biomedical Research, Vol. 8, 1975, pp. 232-243.
14. Pao, Y. C., Ritman, E. L., Robb, R. A., and Wood, E. H.: A Finite-Element Method for Evaluating Cross-Sectional Young's Modulus of Diastolic Left Ventricle. Paper No. F3b.4, The 28th Annual Conference on Engineering in Medicine and Biology, New Orleans, September 20-24, 1975.



Table 1. Comparison of principal stresses for the end-diastolic cross section ( $E=p_1=1$  and  $\nu=0.415$ ).

R E G I O N	Element Number	FEAMPS		NASTRAN			
		Triangular Elements		Triangular Elements		Isoparametric Quadrilateral Elements	
		$\sigma_1$	$\sigma_2$	$\sigma_1$	$\sigma_2$	$\sigma_1$	$\sigma_2$
P O S T E R I O R	425	2.14	-1.16	2.14	-1.16	1.95	-1.30
	426	0.34	-3.15	0.34	-3.15		
	427	9.64	3.53	9.62	3.53	7.50	1.55
	428	4.60	0.12	4.59	0.12		
	429	5.82	1.25	5.81	1.24	7.83	1.05
	430	8.54	0.59	8.53	0.58		
	431	6.41	-1.48	6.40	-1.48	5.80	0.16
	432	4.48	0.34	4.47	0.34		
S E P T A L	439	-0.61	-1.34	-0.61	-1.34	-0.42	-1.15
	440	0.07	-1.06	0.07	-1.06		
	441	-1.06	-1.55	-1.06	-1.55	-1.06	-1.62
	442	-0.76	-1.75	-0.76	-1.74		
	443	-0.88	-1.85	-0.87	-1.84	-1.09	-1.72
	444	-1.05	-1.70	-1.05	-1.69		
	445	-0.03	-1.08	-0.03	-1.07	-0.99	-1.64
	446	-1.16	-1.85	-1.16	-1.85		
A N T E R I O R	453	4.96	0.37	4.95	0.37	6.43	0.08
	454	7.42	-0.99	7.40	-0.99		
	455	7.95	-0.23	7.93	-0.23	6.78	-0.48
	456	5.42	-0.35	5.40	-0.35		
	457	4.88	-0.65	4.87	-0.65	6.64	-0.17
	458	7.62	0.05	7.60	0.04		
	459	5.11	-1.36	5.10	-1.35	4.39	-0.48
	460	3.53	0.22	3.52	0.22		
F R E E	463	-1.40	-2.11	-1.40	-2.11	-1.13	-1.59
	464	0.52	-0.43	0.52	-0.43		
	465	-1.55	-2.21	-1.54	-2.21	-1.11	-1.65
	466	-0.62	-1.58	-0.61	-1.58		
	467	-1.26	-2.10	-1.25	-2.09	-1.20	-1.81
	468	-1.12	-1.73	-1.12	-1.72		
	469	-0.15	-1.11	-0.16	-1.11	-1.04	-1.86
	470	-1.03	-1.97	-1.03	-1.96		

Table 2. Comparison of principal stresses for the early diastolic cross section ( $E=p_1=1$  and  $\nu=0.415$ ).

R E G I O N	Element Number	NASTRAN		FEAMPS			
		$u_6=v_6=v_{19}=0$		$u_6=v_6=v_{19}=0$		No Boundary Constraints	
		$\sigma_1$	$\sigma_2$	$\sigma_1$	$\sigma_2$	$\sigma_1$	$\sigma_2$
P O S T E R I O R	427	5.01	1.44	5.01	1.44	5.01	1.44
	428	2.76	0.48	2.76	0.48	2.76	0.48
	429	1.96	0.30	1.96	0.30	1.97	0.30
	430	7.14	2.73	7.14	2.73	7.14	2.73
	431	5.51	0.06	5.51	0.06	5.51	0.06
	432	0.15	-1.38	0.15	-1.38	0.15	-1.38
	433	1.66	-0.31	1.66	-0.31	1.66	-0.31
	434	2.63	0.11	2.63	0.11	2.63	0.11
S E P T A L	436	0.44	-0.83	0.44	-0.83	0.44	-0.83
	437	-0.10	-1.21	-0.10	-1.21	-0.10	-1.21
	438	-0.11	-0.82	-0.11	-0.82	-0.11	-0.82
	439	-0.81	-1.25	-0.81	-1.25	-0.81	-1.25
	440	0.004	-1.05	0.005	-1.05	0.004	-1.05
	441	-0.01	-1.02	-0.005	-1.02	-0.01	-1.02
A N T E R I O R	442	-0.54	-1.23	-0.54	-1.23	-0.54	-1.23
	443	0.26	-0.71	0.26	-0.71	0.26	-0.71
	446	0.11	-1.59	0.11	-1.59	0.11	-1.59
	447	2.07	-0.01	2.08	-0.10	2.08	-0.10
	448	1.51	-0.97	1.51	-0.97	1.51	-0.97
	449	2.63	-0.17	2.64	-0.17	2.64	-0.17
	450	3.13	-0.96	3.13	-0.96	3.13	-0.96
	451	3.60	-0.49	3.60	-0.49	3.60	-0.49
F R E E	452	2.45	-0.56	2.46	-0.56	2.46	-0.56
	453	2.54	-0.50	2.55	-0.50	2.55	-0.50
	454	4.08	0.02	4.09	0.02	4.09	0.02
	455	2.40	-1.32	2.40	-1.32	2.40	-1.32
	456	1.80	-0.56	1.80	-0.56	1.80	-0.56
	457	0.99	-1.19	0.99	-1.19	0.99	-1.19
	458	1.71	-0.22	1.71	-0.22	1.71	-0.22
	459	0.82	-1.22	0.82	-1.22	0.82	-1.22
460	0.72	-0.88	0.72	-0.88	0.72	-0.88	
461	0.58	-1.07	0.58	-1.07	0.58	-1.07	

Table 3. Comparison of principal stresses for the early and end diastolic cross sections considered as a nearly incompressible material  $\nu=0.49$  ( $E=p_i=1$ ).

R E G I O N	EARLY DIASTOLE				END DIASTOLE			
	FEAMPS		NASTRAN		FEAMPS		NASTRAN	
	$\sigma_1$	$\sigma_2$	$\sigma_1$	$\sigma_2$	$\sigma_1$	$\sigma_2$	$\sigma_1$	$\sigma_2$
P O S T E R I O R	5.69	2.81	5.68	2.81	2.84	0.26	2.67	0.19
	3.87	1.86	3.87	1.85	-0.67	-3.59	-0.64	-3.45
	1.83	-0.08	1.83	-0.09	1.63	-1.40	1.55	-1.37
	8.40	4.65	8.41	4.65	-3.25	-7.33	-3.14	-7.06
	6.96	0.29	6.98	0.29	15.23	10.21	14.56	9.74
	-1.54	-3.42	-1.53	-3.42	-0.15	-4.69	-0.15	-4.50
	2.72	0.68	2.72	0.67	10.31	5.51	9.83	5.22
	3.56	0.84	3.58	0.85	8.74	1.22	8.35	1.14
S E P T A L	0.30	-0.88	0.29	-0.88	5.75	-2.10	5.51	-2.03
	-0.24	-1.45	-0.25	-1.44	6.49	2.56	6.21	2.41
	0.88	-0.44	0.85	-0.45	1.15	-2.52	1.12	-2.43
	-1.57	-3.06	-1.56	-3.03	4.52	0.46	4.38	0.42
A N T E R I O R	2.73	1.24	2.67	1.20	2.17	-1.98	2.19	-1.91
	-0.44	-2.60	-0.45	-2.58	2.01	0.20	1.98	0.16
	3.47	1.10	3.40	1.07	-0.31	-2.04	-0.23	-1.98
	0.30	-2.33	0.26	-2.32	1.48	-0.12	1.52	-0.11
A N T E R I O R	3.76	0.96	3.69	0.94	3.86	1.40	3.80	1.37
	2.84	-1.00	2.78	-1.00	0.19	-3.04	0.28	-2.93
	3.31	-0.38	3.27	-0.38	5.15	1.22	4.99	1.13
	2.40	-0.43	2.34	-0.46	-0.38	-4.51	-0.29	-4.34
A N T E R I O R	2.12	-0.74	2.10	0.73	9.15	4.74	8.83	4.50
	4.09	0.34	4.05	0.22	6.56	-1.20	6.37	-1.19
	2.34	-1.50	2.33	-1.49	7.41	0.08	7.16	0.03
	2.29	0.13	2.27	0.12	4.97	-0.45	4.83	-0.43
F R E E	-0.10	-2.04	-0.10	-2.03	7.54	0.56	7.27	0.51
	1.72	0.10	1.71	0.10	4.31	-1.85	4.16	-1.81
	0.82	-1.35	0.83	-1.35	6.76	3.42	6.54	3.27
	0.91	-0.63	0.91	-0.63	-3.58	-6.32	-3.48	-6.13
F R E E	-0.07	-1.51	-0.06	-1.50	2.75	0.43	2.67	0.41
	-0.05	-1.10	0.06	-1.10	-1.25	-3.12	-1.19	-3.05
	0.45	-0.84	0.46	-0.83	2.59	2.07	2.47	2.00
	1.12	-0.30	1.11	-0.31	-3.14	-3.93	-3.03	-3.82

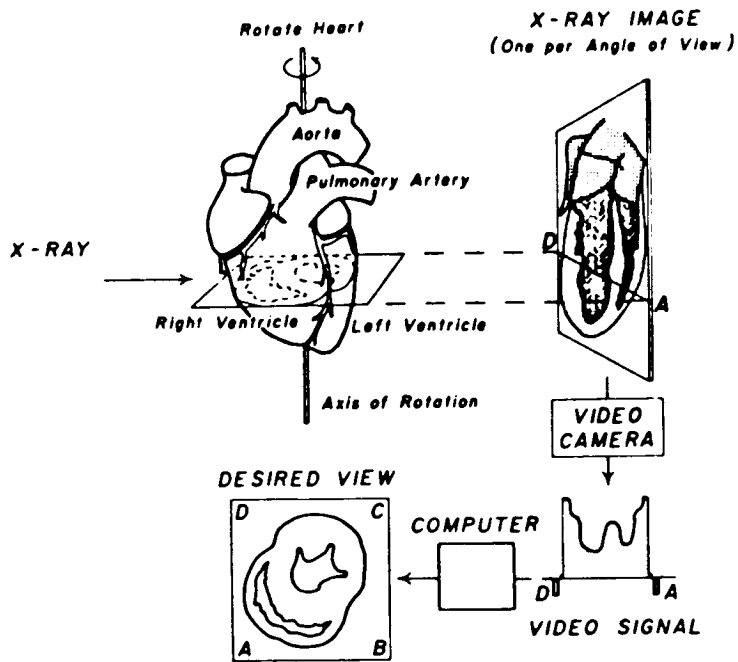


Figure 1. Reconstruction of cardiac cross section from multi-planar x-ray views and by use of algebraic algorithm.

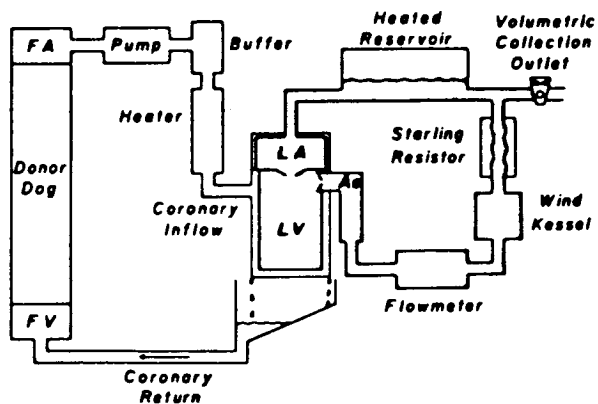


Figure 2. Schematic of the surgically isolated, metabolically supported canine left ventricle.

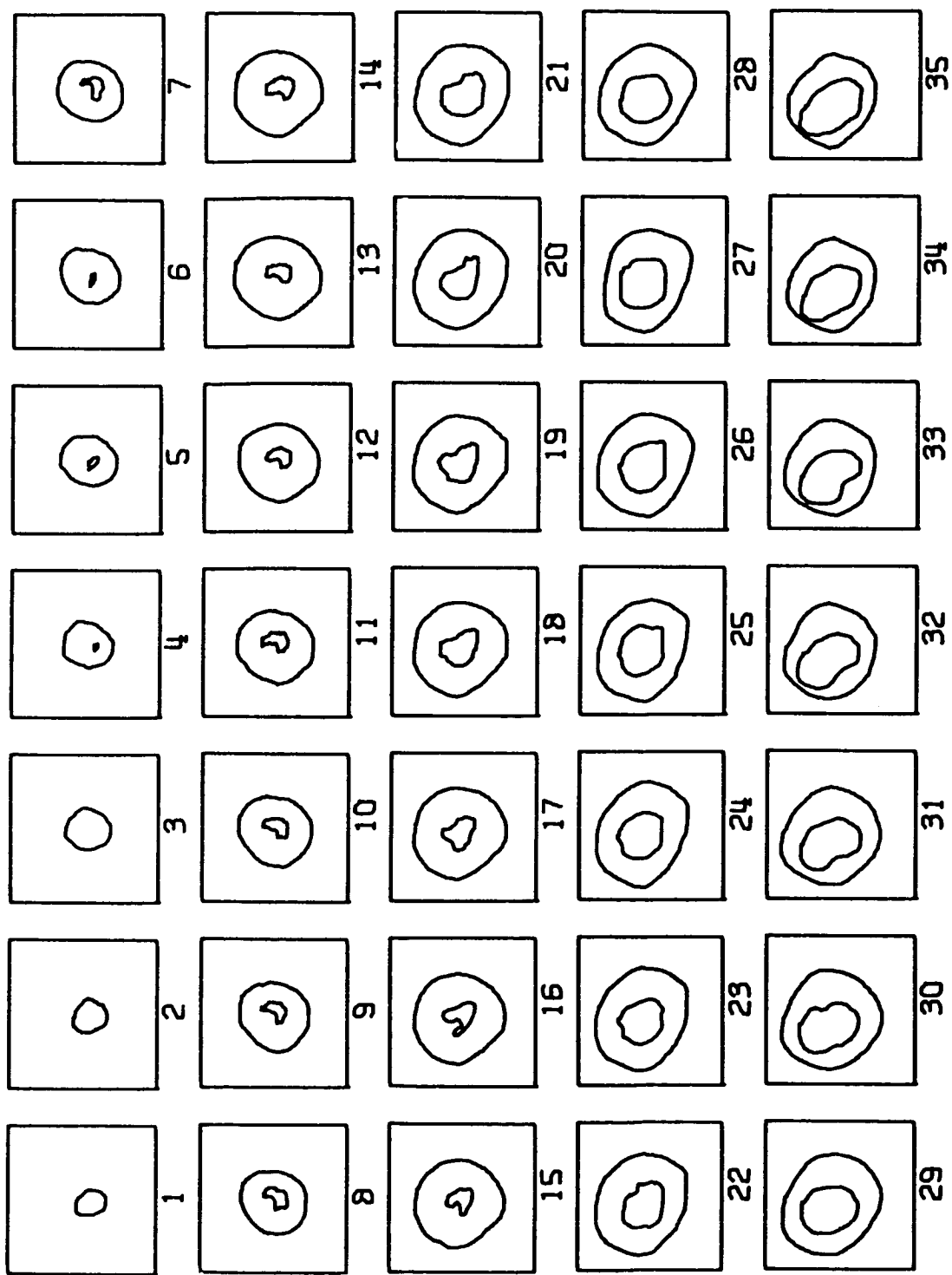


Figure 3. Sample plot of 35 reconstructed apical-to-basal cross sections of an isolated left ventricle during the end of diastole of a cardiac cycle.

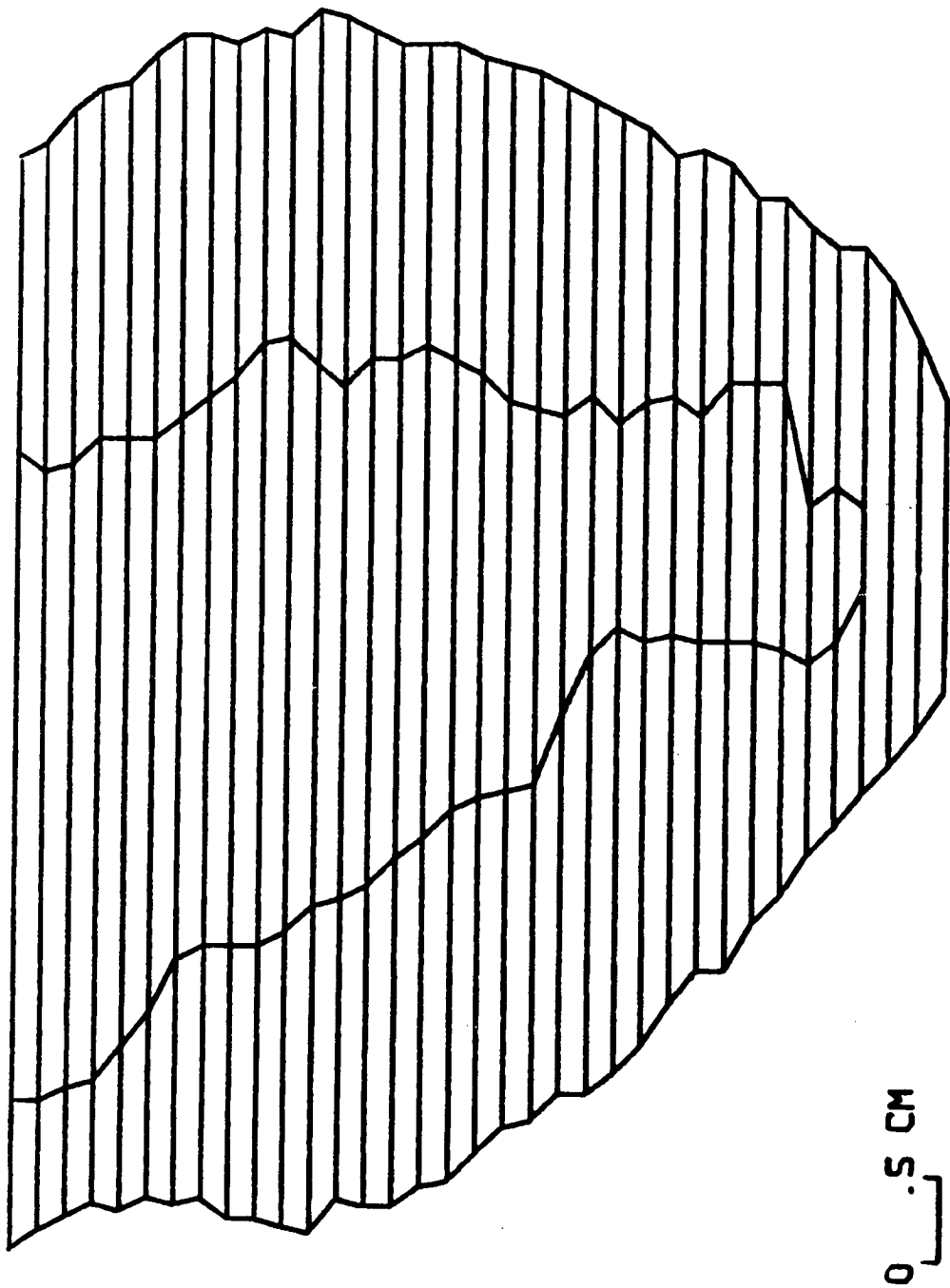
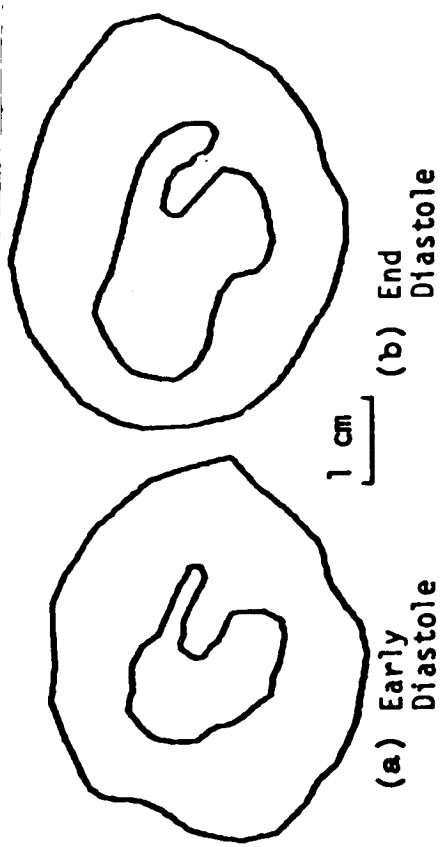


Figure 4. Formation of left ventricular silhouette from stacking the 35 cross sections shown in Fig. 3.



(c) Finite Element Partitioning Pattern

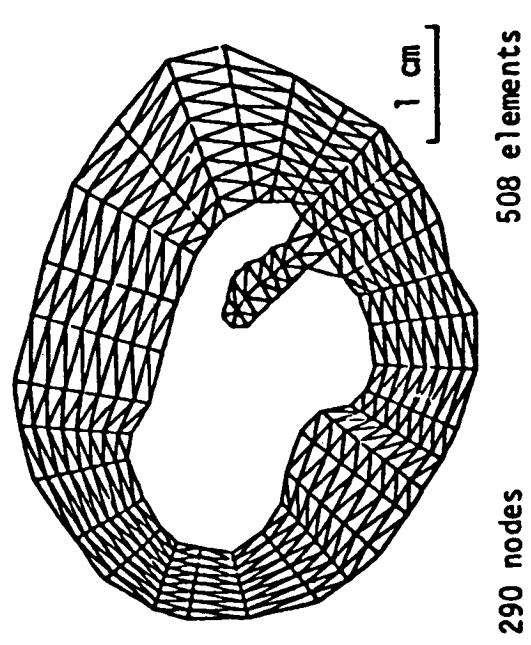


Figure 5. Typical shape and dimension changes of a cross section during diastole, and finite element partitioning pattern.

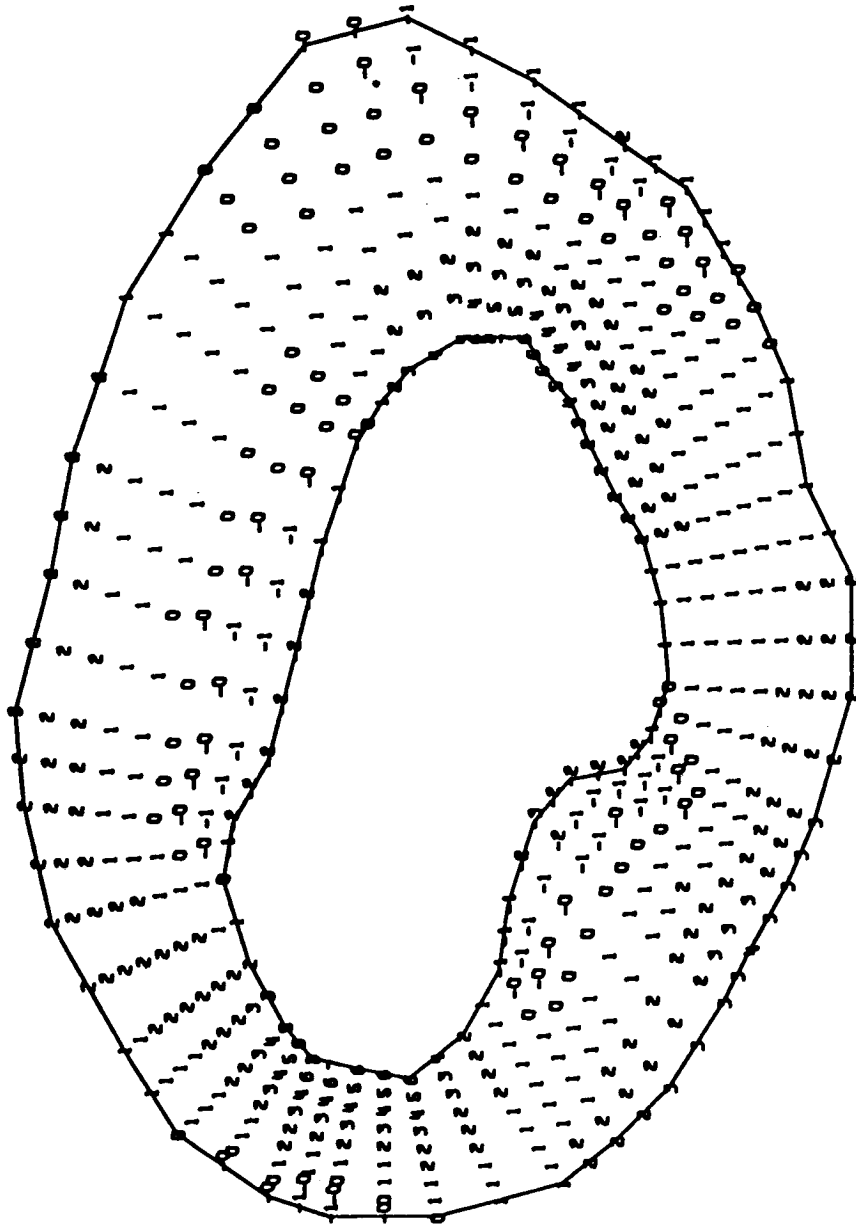


Figure 6. Sample plot of the normalized circumferential stress distribution in an isolated left ventricular cross section.



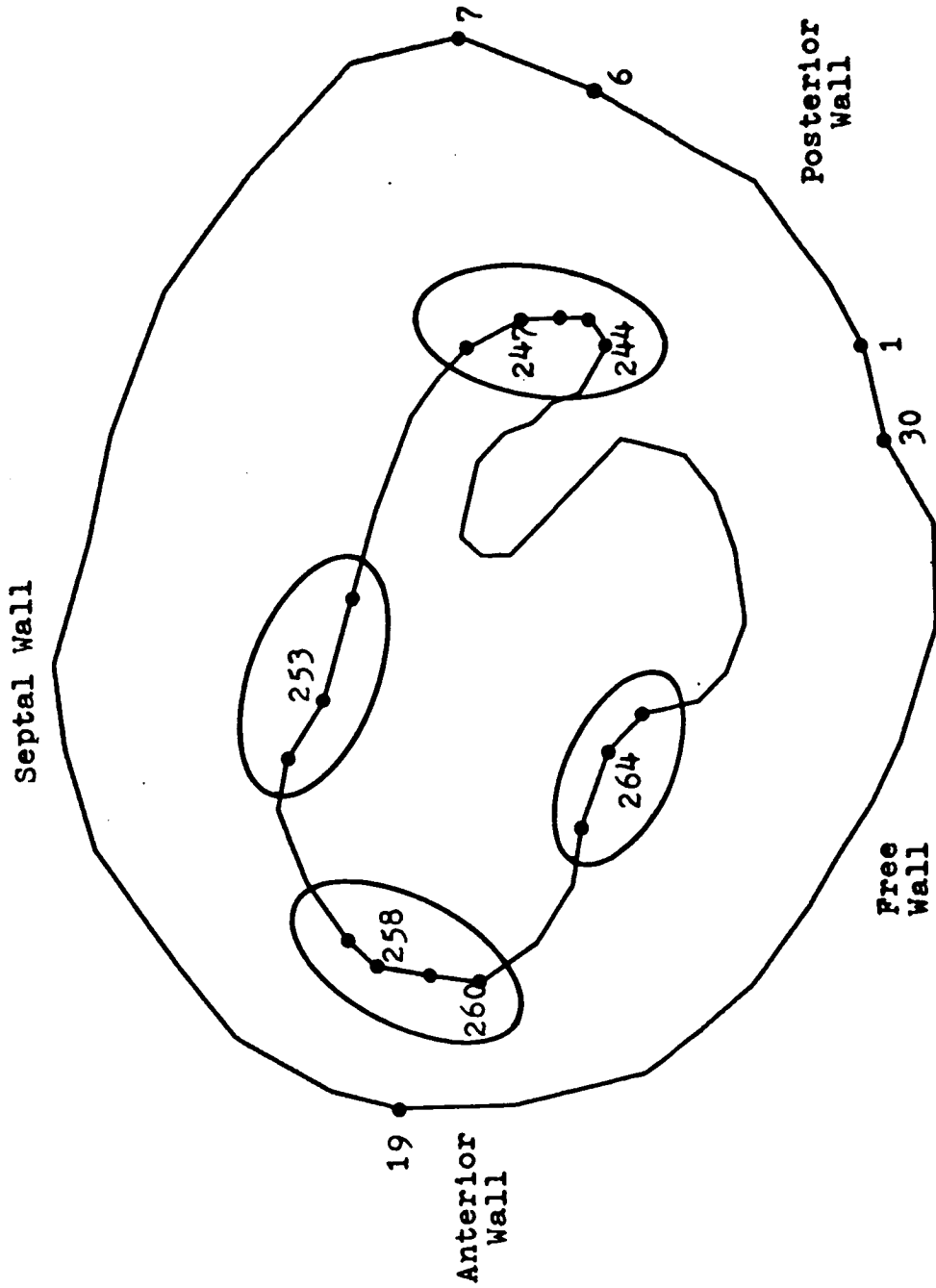


Figure 7. Some node numbers identifying the four regions of extreme stresses.

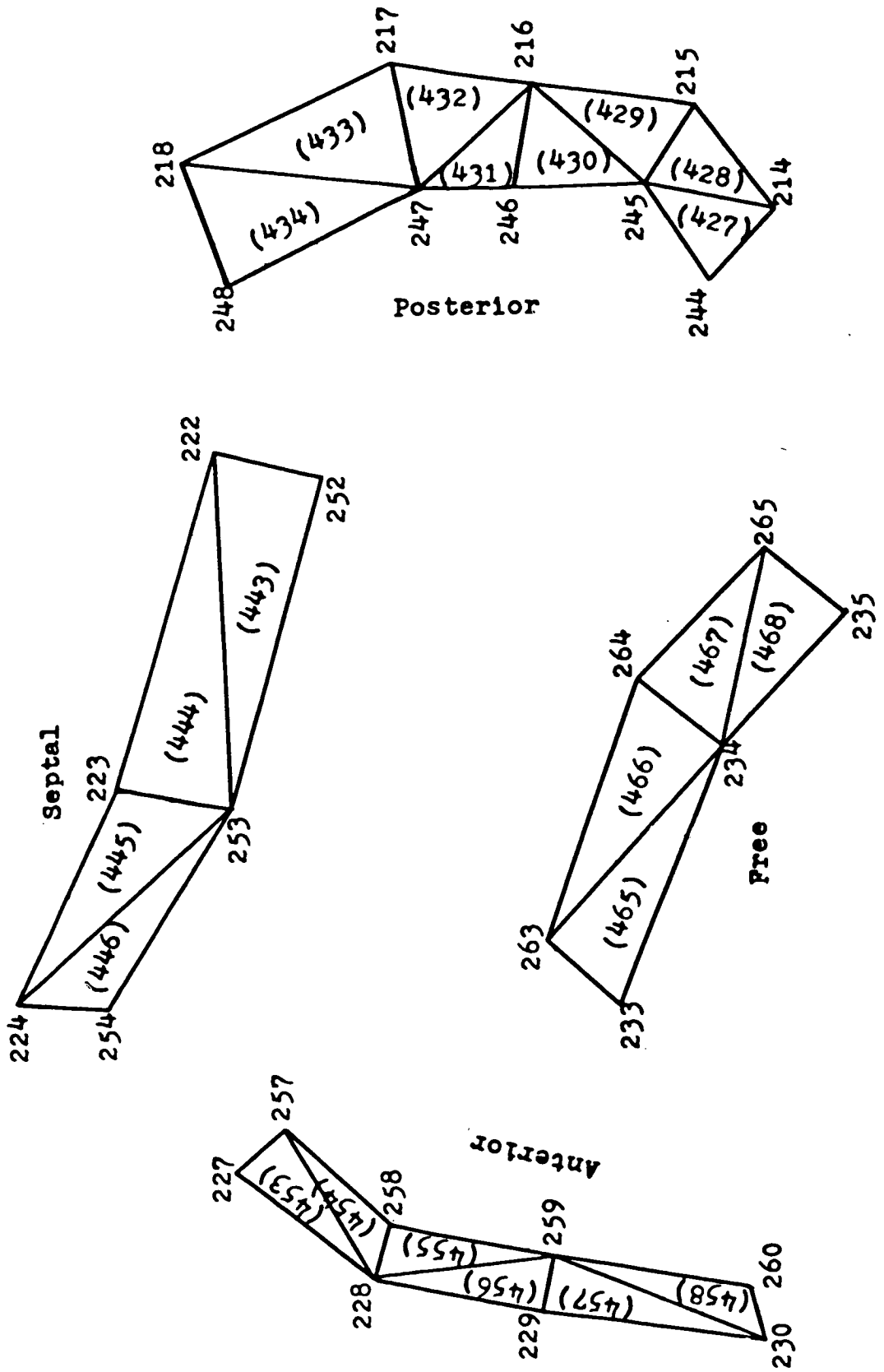


Figure 8. Close-up details of the four regions of extreme stresses with the node and element (parenthetical) numbers indicated.

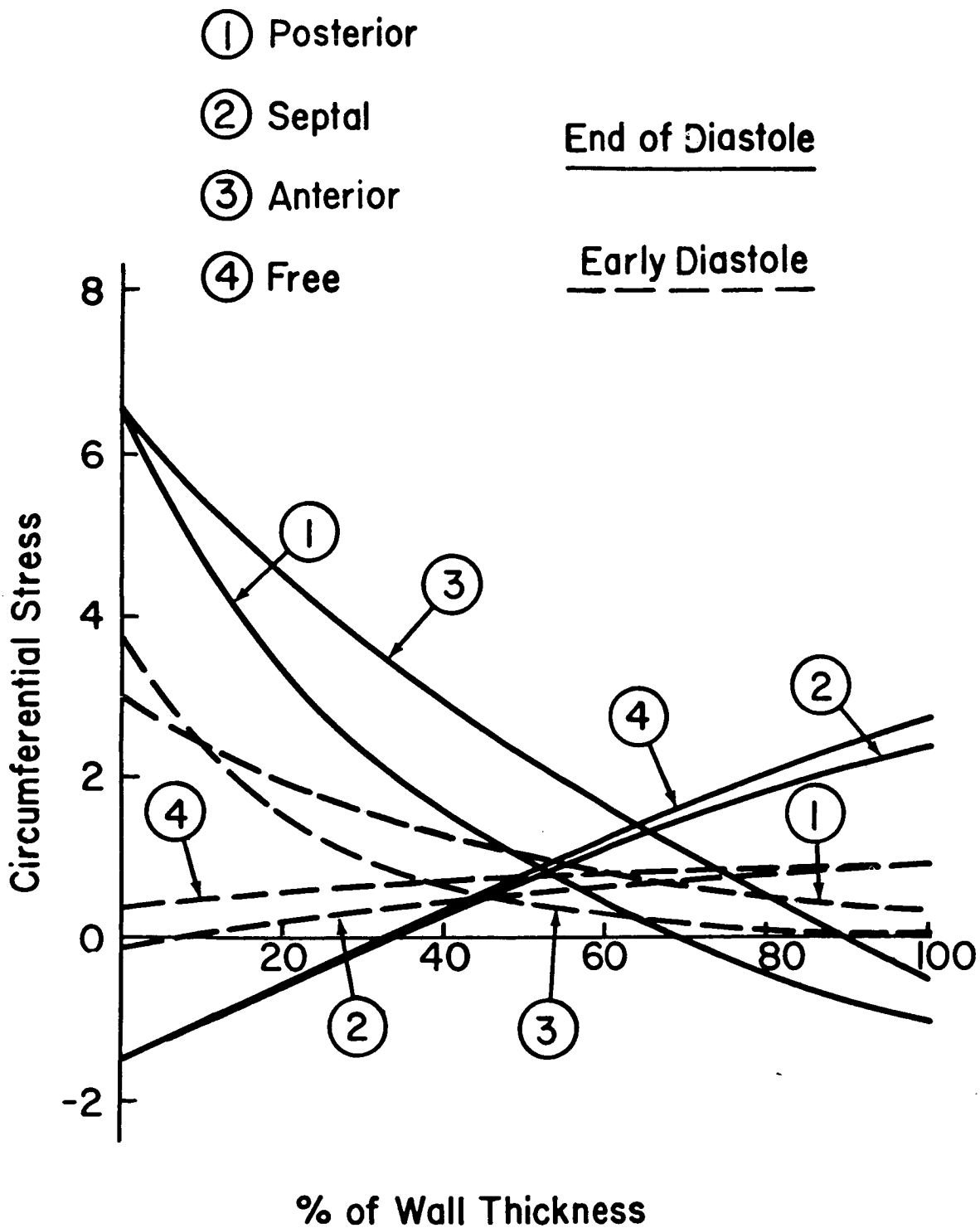


Figure 9. Normalized circumferential stress distributions across the wall thickness at the four regions of the left ventricular cross section.